

Pharmacokinetics, Metabolism, and Disposition of Deferasirox in β -Thalassemic Patients with Transfusion-Dependent Iron Overload Who Are at Pharmacokinetic Steady State

Felix Waldmeier, Gerard J. Bruin, Ulrike Glaenzel, Katharine Hazell, Romain Sechaud, Steve Warrington, and John B. Porter

Novartis Institutes for BioMedical Research, Drug Metabolism and Pharmacokinetics, Basel, Switzerland (F.W., G.J.B., U.G., K.H., R.S.); Hammersmith Medicines Research, Central Middlesex Hospital, London, United Kingdom (S.W.); and University College, London, United Kingdom (J.B.P.)

Received October 16, 2009; accepted January 22, 2010

ABSTRACT:

Deferasirox (ICL670) is a novel once-daily, orally administered iron chelator to treat chronic iron overload in patients with transfusion-dependent anemias. Absorption, distribution, metabolism, and excretion of [14 C]deferasirox at pharmacokinetic steady state was investigated in five adult β -thalassemic patients. Deferasirox (1000 mg) was given orally once daily for 6 days to achieve steady state. On day 7, patients received a single oral 1000-mg dose (~20 mg/kg) of [14 C]deferasirox (2.5 MBq). Blood, plasma, feces, and urine samples collected over 7 days were analyzed for radioactivity, deferasirox, its iron complex Fe-[deferasirox]₂, and metabolites. Deferasirox was well absorbed. Deferasirox and its iron complex accounted for 87 and 10%, respectively, of the radioactivity in plasma (area under the curve at

steady state). Excretion occurred largely in the feces (84% of dose), and 60% of the radioactivity in the feces was identified as deferasirox. Apparently unchanged deferasirox in feces was partly attributable to incomplete intestinal absorption and partly to hepatobiliary elimination of deferasirox (including first-pass elimination) and of its glucuronide. Renal excretion was only 8% of the dose and included mainly the glucuronide M6. Oxidative metabolism by cytochrome 450 enzymes to M1 [5-hydroxy (OH) deferasirox, presumably by CYP1A] and M4 (5'-OH deferasirox, by CYP2D6) was minor (6 and 2% of the dose, respectively). Direct and indirect evidence indicates that the main pathway of deferasirox metabolism is via glucuronidation to metabolites M3 (acyl glucuronide) and M6 (2-O-glucuronide).

In patients with transfusion-dependent anemias, toxic and potentially lethal levels of iron accumulate over time. Humans are unable to actively eliminate iron from the body, once it has been acquired. Toxic and eventually lethal levels of iron accumulate as a result of repeated transfusions, e.g., in β -thalassemia major, or because of excessive dietary iron uptake in anemias and hereditary hemochromatosis (Barton, 2007). The harmful effects of chronic iron overload can lead to damage of the liver, heart, and endocrine glands, resulting in organ compromise and death. For the last 40 years, deferoxamine (Desferal) has been the standard of care for removal of excess body iron. The poor oral bioavailability and the short plasma half-life of deferoxamine necessitate its administration as slow subcutaneous or intravenous infusions. As a result, the most common difficulty asso-

ciated with long-term deferoxamine is erratic compliance with therapy (Kushner et al., 2001). The need for an iron chelator that can be given orally has been recognized for a long time.

Deferasirox (ICL670, Exjade; Novartis Pharma AG, Basel, Switzerland) is a potent and specific iron chelator, recently approved as first-line therapy for blood transfusion-related iron overload; it binds Fe³⁺ in a 2:1 ratio (Nick et al., 2002). The recommended initial daily dose is 20 mg/kg b.wt., rounded to the nearest available tablet strength; the currently recommended maximal dose is 30 mg/kg/day (Yang et al., 2007). Deferasirox is administered orally as a suspension after dispersion in water or orange or apple juice, whereby the degree of dispersion does not affect the bioavailability of deferasirox (Séchaud et al., 2008a).

Pharmacokinetics, metabolism, and disposition of deferasirox have been investigated in mouse, rat, and marmoset using nonradiolabeled and 14 C-radiolabeled deferasirox. The disposition of deferasirox in rats was published recently (Bruin et al., 2008). In general, orally dosed deferasirox was well absorbed, and peak plasma concentrations of deferasirox and radioactivity (metabolites) were reached within 0.5 to 1 h. Part of the dose was excreted unchanged, mainly in the feces (via bile), and part was metabolized to an acyl glucuronide. Four hydroxylated metabolites were formed by oxidative metabolism

Parts of this work were previously presented at the following conference: Porter JB, Waldmeier F, Bruin G, Shah F, Hazell K, Warrington S, Delage S, Séchaud R, Peter R, Ford J, Alberti D, Gross G, and Schran H (2003) Pharmacokinetics, metabolism and elimination of the iron chelator drug ICL670 in β -thalassemia patients. *Blood (ASH Annual Meeting Abstracts)* **102(11, part 2)**: Abstract 3720.

Article, publication date, and citation information can be found at <http://dmd.aspetjournals.org>.

doi:10.1124/dmd.109.030833.

ABBREVIATIONS: ICL670, deferasirox; ADME, absorption, distribution, metabolism and excretion; OH, hydroxy; HPLC, high-performance liquid chromatography; LOQ, limits of quantitation; LSC, liquid scintillation counting; LC, liquid chromatography; MS, mass spectrometry; AUC, area under the curve; P450, cytochrome P450; MRP/Mrp, multidrug resistance protein.

(phase I metabolism). Those metabolites were subsequently metabolized to *O*-glucuronides or *O*-sulfates and then excreted, mainly via bile and feces. The metabolites were suspected to retain the ability to form iron complexes. Therefore, the 3-hydroxy and the 5-hydroxy metabolites were synthesized and administered to rats, but they were shown to contribute little to the iron elimination (Bruin et al., 2008). In investigations *in vitro*, the oxidative metabolism of deferasirox was found to be catalyzed mainly by the cytochrome P450 enzymes CYP1A1 and CYP1A2. A minor metabolite was formed by CYP2D6 (reference data on file, see Bruin et al., 2008). In metabolism studies *in vitro*, the same metabolic pathways were observed in liver microsomal fractions from several animal species and humans. On the basis of those studies, the metabolism and disposition of deferasirox in humans were expected to be similar to those observed in animals. However, we could not predict which metabolism and elimination pathways would be of quantitative importance. Therefore, this radiolabeled absorption, distribution, metabolism, and excretion (ADME) study was done to investigate the fate of deferasirox in human subjects, i.e., pharmacokinetics, mass balance, and metabolism of deferasirox, to define the biotransformation, transport, and clearance mechanisms involved in the disposition of deferasirox. In general, human ADME studies are done in healthy volunteers with administration of a single dose. In the present case, due to the iron elimination effect of deferasirox, it was deemed better to do the study in patients with thalassemia. Thus, patients undergoing treatment with deferoxamine had to switch treatment to deferasirox, and oral dosing had to be continued to achieve steady state, which is the ideal scenario for a human ADME study.

Materials and Methods

Nonradioactive Deferasirox. Deferasirox (4-[3,5-bis-(2-hydroxy-phenyl)-[1,2,4]triazol-1-yl]-benzoic acid, C₂₁H₁₅N₃O₄, molecular weight 373.4) was synthesized at the Novartis Institute for Biomedical Research (Basel, Switzerland).

¹⁴C-Radiolabeled Deferasirox. The radiolabeled drug [¹⁴C]deferasirox was synthesized by the Isotope Laboratory of Novartis Pharma AG. The radiolabel was in the C-3 and C-5 positions of the central triazole ring (see structural formula in Table 3). The parent batch was diluted down to the final specific activity using a nonradiolabeled good manufacturing practice drug substance batch, which had been released for human use, and analyzed for release for human use according to predefined specifications. Radiochemical purity was >98% with a specific radioactivity of 2.534 kBq/mg (0.0684 μCi/mg).

Reference Compounds and Other Materials. For comparison with metabolites, the following reference compounds were synthesized by Novartis Institute for Biomedical Research: 5-OH derivative of deferasirox (M1) and 5'-OH derivative of deferasirox (M4). Solvents and reagents, all of analytical grade, were purchased from commercial manufacturers.

Pooled rat cryopreserved hepatocytes and human cryopreserved hepatocytes from a male donor were purchased from In Vitro Technologies (Baltimore, MD). HepatoZYME-SFM medium and Hanks' balanced salt solution with Ca²⁺ or Mg²⁺ (10×) were purchased from Invitrogen (Carlsbad, CA). Percoll (colloidal polyvinylpyrrolidone-coated silica) was obtained from GE Healthcare Bio-Sciences (Uppsala, Sweden).

Subjects and Design of Study. The study enrolled five patients (3 male and 2 female) with an age range from 20 to 38 years, a body weight range from 50 to 81 kg, and a height range from 153 to 165 cm. All five patients completed the study.

This was an open-label study in patients with β-thalassemia. They had received subcutaneous deferoxamine to treat transfusion-dependent iron overload. After screening, patients discontinued deferoxamine treatment for 5 days (iron chelation-free period, washout phase). Subsequently the patients commenced 6 days of treatment with oral deferasirox at a dose of 1000 mg/day (approximately 20 mg/kg) once daily. The patients received a single oral nominal dose of 1000 mg of [¹⁴C]deferasirox (2.6 MBq, 70 μCi) on day 7, i.e., at steady state (Nisbet-Brown et al., 2003). Because the

actual doses were within a minimal range and within weighing precision, the nominal dose of 1000 mg was taken as a basis for mass balance calculation. The observation and sample collection period (blood, plasma, urine, and feces) was 168 h. Four of the five patients continued to receive daily doses of standard deferasirox from day 8 to the end of the study. For one patient the standard dose of deferasirox was withheld for the rest of the study, but his sample collection was also continued up to 168 h. At the end of the study, all five patients were switched back to parenteral deferoxamine, as determined by the investigator.

Radiation Protection. The radiation exposure of the patients was estimated prognostically, based on the available animal ADME and human pharmacokinetics data and according to the guidelines of the International Commission on Radiological Protection. The radiation dose (whole-body dose, "effective dose") taken up by the patients was estimated to be 0.89 mSv. Radiation dosimetry calculations and the study protocol were approved by the UK Administration of Radioactive Substance Advisory Committee.

Ethics. The study was approved by the local ethics committee. Written informed consent was obtained from each subject before enrollment.

Sample Collection. After a predose sample (0 h) and radiolabeled dose administration, blood samples were collected at 0.5, 1, 1.5, 2, 3, 4, 6, 8, 12, 24, 48, 72, 96, 120, 144, and 168 h postdose into heparinized tubes. Blood samples were taken by either direct venipuncture or via an indwelling cannula inserted into a forearm vein. Sample volumes per time point ranged from 5 to 12 ml. Three aliquots of 0.3 ml were removed and weighed in counting vials for radioactivity determination in blood. The remaining blood was centrifuged to obtain plasma for radioactivity determination, analysis of deferasirox and its iron complex Fe-[deferasirox]₂ (cold analysis), analysis of metabolite patterns, and metabolite structure elucidation. Predose blank urine was collected on day 7 and predose blank feces on day 5 or 6. After the radiolabeled dose, quantitative collections of urine were done over the whole period from dosing to 168 h, in the time intervals 0 to 6, 6 to 12, 12 to 24, 24 to 48, 48 to 72, 72 to 96, 96 to 120, 120 to 144, and 144 to 168 h postdose. All and complete feces portions were collected over the period 0 to 168 h.

Sample Storage and Shipment Conditions. After sample collection, blood, plasma, urine, and feces samples were frozen immediately and stored at ≤ -18°C until and after analysis in the analytical laboratories. Stability of deferasirox, of its iron complex, and of the metabolites was ascertained under those conditions. Samples were shipped to other analytical laboratories under dry ice.

Analysis of Deferasirox and Its Complex Fe-[Deferasirox]₂. Concentrations of the parent drug deferasirox, deferasirox iron complex in plasma, and total deferasirox (i.e., free ligand and iron complex) in urine were measured quantitatively by a validated specific assay based on HPLC with UV detection (Rouan et al., 2001). The lower limits of quantification (LOQ) in plasma were 1.34 and 0.314 μM for deferasirox and the deferasirox iron complex, respectively. The lower LOQ for deferasirox in urine was 0.670 μM. The sample volume was 100 μl for both plasma and urine. Measurements below the LOQ were not considered in the calculation of means and were reported as zero.

In genuine plasma samples, it was shown that the Fe-[deferasirox]₂ complex was stable in the presence of an excess of deferasirox (Rouan et al., 2001). The Fe-[deferasirox]₂ is stable at neutral pH, whereas it tends to dissociate at acidic pH; therefore, the HPLC was run with a mobile phase of pH 7. Addition of the ion pair reagent tetrabutylammonium hydrogen sulfate allowed the separation of deferasirox and Fe-[deferasirox]₂ complex. Furthermore, the acetonitrile content in the mobile phase was kept at only 10% and the methanol content at 48%, because higher percentages of acetonitrile led to dissociation of the complex during the chromatographic run.

Radioactivity Analysis of Blood, Plasma, Urine, and Feces Samples. Determination of ¹⁴C radioactivity in blood, plasma, urine, and feces samples was done by liquid scintillation counting (LSC) with a typical counting time of 10 min using a Tri-Carb 2000CA liquid scintillation counter (PerkinElmer Life and Analytical Sciences, Waltham, MA) at RCC Ltd. (Itingen, Switzerland). Low levels in blood and plasma were counted for 30 min. Blood and plasma samples (triplicates of 300 μl each, weighed) were counted after solubilization. Feces samples (quadruplicates of 400 mg each, weighed) were counted after combustion in a sample oxidizer. Urine samples (duplicates of 1 ml each) were measured directly, after addition of scintillation cocktail (see below).

Radioactivity in pooled feces homogenates and in pellets from extractions for metabolism investigations, were measured after solubilization with Soluene 350 (PerkinElmer Life and Analytical Sciences) and addition of 4 ml of liquid scintillation cocktail OptiPhase HiSafe 3 (PerkinElmer Life and Analytical Sciences). Urine samples, plasma samples, and feces extracts were measured directly after addition of 4 ml of LSC cocktail using standard counting procedures. Quench correction was done by the external standard method. The LOQ for each matrix was calculated as described elsewhere (Jost et al., 2006; Waldmeier et al., 2007). It was defined as the minimum number of disintegrations that was statistically significantly above background and that showed a relative statistical uncertainty $\leq 20\%$. The LOQ was 9 and 10 dpm for blood and plasma, respectively (counting time 30 min), corresponding to concentrations of 0.5 to 0.6 μM . For urine, the LOQ was 20 dpm (500 nmol, approximately 0.02% of the dose). For feces the LOQ was 17 dpm (200 nmol, approximately 0.01% of the dose).

Radioactivity Analysis of Collected HPLC Fractions. For HPLC radiochromatograms, 50- μl HPLC fractions (15-s fractions) were collected into Deepwell Lumaplates (PerkinElmer Life and Analytical Sciences) using a fraction collector (Gilson FC204; Gilson Inc., Middleton, WI). After evaporation of solvent in a Savant SpeedVac AES2010 (Thermo Fisher Scientific, Waltham, MA), the plates were counted in a Packard TopCount NXT Microplate Scintillation and Luminescence Counter as described previously (Bruin et al., 2006).

Sample Preparation of Plasma, Urine, and Feces for Metabolite Investigation. Semiquantitative determination of main and trace metabolites by radio-HPLC with offline microplate solid scintillation counting and structural characterization by LC-MS was done in plasma, urine, and feces. Aliquots of 200 μl of plasma samples collected at 1.5, 4, 6, 8, 12, and 24 h after dosing were diluted 2-fold with 25 mM ammonium formate with 2.5 mM EDTA, pH 5.5, and centrifuged. Aliquots of 50 μl were analyzed for radioactivity by LSC. The recovery was 100%. Volumes of 200 μl of the diluted plasma were injected into the HPLC. The recovery of radioactivity after HPLC, as a percentage of the amount injected, was determined in a separate run in which the whole eluent was collected. Recovery from HPLC was approximately 100%. From the urine collected over 72 h, aliquots were pooled per subject. The 0- to 72-h pools represented 97 to 100% of the total excreted radioactivity in urine in the time period 0 to 168 h. The urine pools were centrifuged at 2860g for 10 min. The recovery of radioactivity after sample processing was 100%. Volumes of 200 μl of the undiluted urine pools were analyzed by HPLC. The recovery of radioactivity from HPLC was approximately 100%. Feces pools were prepared for each subject, combining the most important feces portions such that 97 to 100% of the total radioactivity excreted in feces in the period 0 to 168 h was included, i.e., feces portions with marginal radioactivity contents were excluded to avoid dilution. Approximately 2 g of pooled feces homogenate was extracted with 4 ml of acetonitrile-water (1:1, v/v), by shaking gently for 30 min. Thereafter, the suspension was centrifuged for 20 min at 2700g (Minifuge RF; Heraeus, Sepatech, Osterode, Germany). The pellet was extracted once again with 2 ml of acetonitrile-water (1:1; v/v) by shaking for 30 min followed by centrifugation. The supernatants were combined, and three aliquots of 200 μl were taken for determination of radioactivity recovery by LSC. The recovery was between 85 and 94% except for one subject (67%). Volumes of 100 μl of the feces extracts were analyzed by HPLC. The recovery from HPLC was 100%.

HPLC Instrumentation for Metabolite Pattern Analysis. HPLC method. The HPLC system consisted of two HPLC micro pumps (model PU-1580; Jasco, Tokyo, Japan) with a high-pressure gradient mixer (75 μl). Sample volumes between 50 and 200 μl were injected manually. The chromatogram was monitored by UV detection at a wavelength of 235 nm. The software used was Jasco-Borwin (version 1.50; Omnilab AG, Mettmenstetten, Switzerland). For profiling of metabolite patterns, samples were analyzed on a 250 \times 2 mm i.d. LiChrospher 100-5 RP18 ec HPLC column (particle size 5 μm , pore size 100 \AA , end-capped; Macherey-Nagel, Oensingen, Switzerland), protected by a 4 \times 2 mm i.d. LiChrospher 100-5 RP18 ec guard column (particle size 5 μm , pore size 100 \AA , end-capped; Macherey-Nagel) and maintained at 20°C in a column heater/chiller (model 7955; Jones Chromatography, Hengoed, Mid Glamorgan, UK). The components were eluted with a gradient of 25 mM ammonium formate with 2.5 mM EDTA, pH 5.5 (mobile phase A) and

acetonitrile (mobile phase B) at a flow rate of 0.2 ml/min. HPLC fractions were collected for off-line radioactivity detection as described above.

Evaluation of HPLC data. The amounts of metabolites or parent drug in plasma or excreta were derived from the radiochromatograms by dividing the radioactivity eluting from the HPLC column, which is equal to radioactivity in the original sample minus losses from sample preparation and HPLC, by the relative peak area. Parent drug or metabolites were expressed as micromolar concentrations in plasma or as percentage of dose in excreta. Those values are only semiquantitative compared with those determined by the validated quantitative HPLC-UV assay. Under the conditions of sample preparation and under optimized HPLC conditions for a complete separation of metabolites, with a mobile phase pH 5.5 and acetonitrile as organic modifier in the mobile phase, with long run times, and without ion-pair reagent, the iron complex dissociated. The Fe-[deferasirox]₂ complex could therefore not be measured by the HPLC method used for the metabolite patterns, and the [¹⁴C]deferasirox peak included drug substance that had been present in the form of the complex.

Structural Characterization of Metabolites. Urine pools, feces pool extracts, and incubations of feces pool extracts and isolated metabolites from urine with β -glucuronidase/arylsulfatase were analyzed by LC-MS. HPLC analysis was as described above, except that the mobile phase did not include EDTA. The HPLC effluent was split in a ratio of approximately 1:3. A quarter of the effluent (50 $\mu\text{l}/\text{min}$) was directed into the electrospray LC-MS interface of a Finnigan LCQ-Deca XP ion trap mass spectrometer (Thermo Fisher Scientific). The remaining effluent was directed into a flow-through Packard scintillation analyzer (500TR series; PerkinElmer Life and Analytical Sciences). The electrospray interface was operated with nitrogen as the sheath gas at 150 psi. The transfer capillary temperature was 270°C. The spray voltage was 4.8 kV. Positive ion mode spectra with in-source fragmentation at 0, 25, 45, and 70 V were recorded. To protect the mass spectrometer from nonvolatile salts and other early eluting components, the divert valve before the LC-MS interface was switched to waste during the first 2 min of each run.

Besides the use of LC-MS for structure characterization, isolated metabolite M7, urine, and a feces pool extract were treated enzymatically. To obtain enough metabolite M7 to be characterized, 1 ml of a 0- to 6-h urine fraction was manually injected into the HPLC system described below, which was essentially the same as that for the metabolite patterns, but with an HPLC column diameter of 4 mm and an online radioactivity detector (flow-through detector Berthold 506 C with a Z-500-U4M admix cell of 500 μl ; Berthold, Wildbad, Germany).

Metabolite M7 (peak eluting at a retention time of approximately 35 min) was collected, and the eluent concentrated by evaporation (Eppendorf concentrator 5301; Vaudaux-Eppendorf, Schönenbuch, Switzerland) under reduced pressure to a final volume of approximately 100 μl . The stability of the metabolite during isolation and evaporation was investigated by LC-MS of 30 μl of the collected and preconcentrated metabolite.

Volumes of 30 μl of isolated and preconcentrated metabolite M7 or urine were subjected to enzymatic cleavage at 37°C for 15.5 h with 10 μl of crude enzyme mixture, containing β -glucuronidase/arylsulfatase from *Helix pomatia* (Roche Diagnostics, Mannheim, Germany) in 160 μl of sodium acetate buffer at pH 5.12 (total incubation volume 200 μl). After incubation, the incubate was centrifuged in a Desaspeed LC-1K (Desaga GmbH, Wiesloch, Germany) at 9000 rpm for 15 min and evaporated to a final volume of approximately 50 μl . Then, 50 μl of 25 mM ammonium formate, pH 5.3, was added, and 100 μl was analyzed by LC-MS with radioactivity detection.

A volume of 300 μl of feces homogenate was mixed with 300 μl of phosphate buffer at pH 5.2 and subjected to enzymatic cleavage at 37°C for 92 h with a 120 μl of mixture of β -glucuronidase/arylsulfatase from *H. pomatia* (total incubation volume 720 μl). After incubation, analysis was as above.

Studies with Cryopreserved Rat and Human Hepatocytes. Cells were stored in liquid nitrogen until use. Immediately before use, vials of hepatocytes (1 ml) were thawed and mixed with the serum-free medium HepatoZYME-SFM, Percoll, and 10 \times Hanks' balanced salt solution (18:9:1, v/v/v). The cells were centrifuged at 173g for 20 min at room temperature, and the pellet was resuspended in HepatoZYME-SFM. The cell number and viability were determined by trypan blue exclusion assay before drug incubations. [¹⁴C]Deferasirox was incubated at a concentration of 50 μM in 12-well plates containing human hepatocyte suspensions (1.2 million cells/ml, viability 62%) or rat hepatocyte suspensions (1.3 million cells/ml, viability 70%) in a gassed incu-

bator (5% CO₂) at 37°C for 3 h. Control samples without hepatocytes were also run. In the samples taken at 3 h, the metabolic reactions were stopped by addition of the same volume of acetonitrile-formic acid (95:5, v/v). Samples were subsequently frozen for at least 15 min at -20°C and then centrifuged at 20,000g for 10 min at 4°C. The supernatants were diluted 1:3 (v/v) with 25 mM ammonium formate with 2.5 mM EDTA, pH 5.6, for HPLC and LC-MS analysis.

Aliquot volumes up to 300 µl were analyzed by either HPLC or LC-MS coupled to online radioactivity detection. All HPLC and LC-MS runs were done using an 1100 Agilent HPLC system (Agilent Technologies, Waldbronn, Germany). Separation was achieved with the same chromatographic conditions as described above. For online radioactivity detection with HPLC and in parallel to mass spectrometry the effluent was mixed with 0.6 to 0.8 ml/min Rialuma liquid scintillation cocktail (Lumac, Groningen, The Netherlands) before it entered the radiomonitor flow scintillation analyzer (Packard 500TR series, 100 µl flow cell; PerkinElmer Life and Analytical Sciences). Mass spectrometric analysis was performed by using the same mass spectrometer and similar mass spectrometric conditions as those described above.

Enzymatic hydrolysis was performed by incubation with β-glucuronidase/arylsulfatase as described above. Alkaline hydrolysis was done in Borax-NaOH buffer (Fluka, Basel, Switzerland) at pH 10 for 22 h (37°C). Control incubations without the enzyme mixture or the alkaline buffer were done to determine the stability of the sample over the incubation time. Subsequently the samples were centrifuged and subjected to HPLC analysis with radioactivity detection as described above.

Pharmacokinetic Evaluation. Pharmacokinetic parameters were calculated using noncompartmental methods. The apparent terminal half-life $t_{1/2\lambda z}$ was determined from the slope of the regression line of $\ln(C_t)$ versus time t . For calculation of $t_{1/2\lambda z}$, blood and plasma concentrations were used, which were measured in the time period shown in the data tables. The AUC_t is the area under the concentration-time curve from time 0 to the indicated time point (typically last measurable time point), calculated by the linear trapezoidal method. AUC is the area under the concentration-time curve from time 0 to infinity, calculated as $AUC_t + C_t \cdot t_{1/2\lambda z} / \ln 2$, where C_t is the concentration at time t of last measurable concentration. Descriptive statistical evaluation of pharmacokinetic parameters included means and SD.

The binding of total radioactivity in whole blood to red blood cells was calculated as $F_{RBC} (\%) = 100 \times [1 - (C_p \times (1 - H)/C_b)]/H$ (Hinderling, 1997), where $F_{RBC} (\%)$ is the fraction of total radioactivity bound to red blood cells, C_p is the concentration of radioactivity in plasma, measured at day 8 at 24 h after radiolabeled dose administration, C_b is the concentration of radioactivity in whole blood, measured at day 8 at 24 h after radiolabeled dose administration, and H is the hematocrit, determined at day 8 at 24 h after radiolabeled dose administration.

Results

Safety and Tolerability. All five enrolled patients completed the study with no serious adverse events. On days 8 to 9 of the study (1–2 days after the last dose of deferasirox) three of the five patients developed a maculopapular skin rash, two of mild and one of moderate severity. The skin rash in two of these patients was accompanied by mild pruritus. The two remaining patients experienced mild pruritus without an accompanying skin rash. These adverse events were suspected to be related to the study drug and had either resolved or improved by the end of the study. Headaches in two of five patients, leg pain, and dyspepsia (all of mild severity) were also suspected to be drug-related. All adverse events that were not suspected to be drug-related were of mild severity.

Pharmacokinetics in Plasma. Before administration of a single oral dose of [¹⁴C]deferasirox, the treatment of the patients was switched from intravenous deferoxamine to once-daily oral dosing with deferasirox to pharmacokinetic steady state. Steady state was reached by day 7 according to Nisbet-Brown et al. (2003). At time 0 on the day of radiolabeled dose administration, “cold” deferasirox was present in plasma at trough levels of approximately 20 µM, as determined by a quantitative HPLC-UV assay. Further-

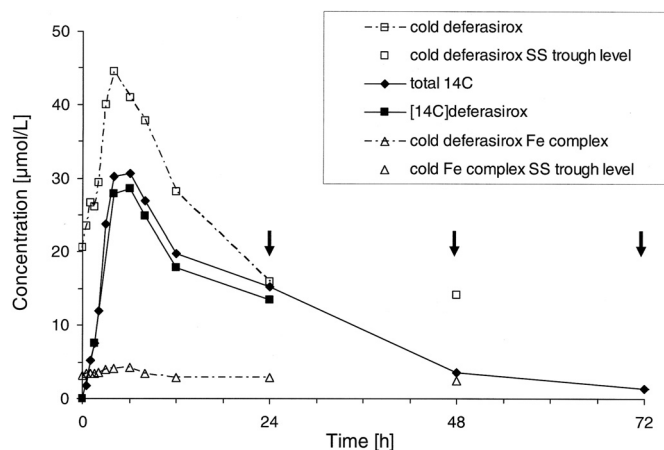


Fig. 1. Mean plasma concentrations of total ¹⁴C radioactivity, deferasirox (cold), Fe-complex (cold), and [¹⁴C]deferasirox (means of $n = 5$). Nonlabeled deferasirox was administered before the radiolabeled dose (pretreatment to steady state) and every 24 h after the radiolabeled dose (arrows). Open symbols, steady-state levels of deferasirox and Fe-complex, respectively, determined by “cold” assay; filled symbols, total radioactivity and the radioactivity fraction represented by [¹⁴C]deferasirox.

more, by a separate, specific, radioactivity-based assay, the plasma levels of [¹⁴C]deferasirox were determined after radiotracer dose administration. The combined measurements (means) are depicted in Fig. 1. The t_{max} values were very similar for cold and radiolabeled deferasirox as well as for total radioactivity, with medians in the range from 4 to 6 h (Table 1), which indicates a rather slow absorption. In two patients, a second, lower maximum or shoulder was observed at 24 h after dose, which probably indicates some enterohepatic recirculation of deferasirox.

Radioactivity in plasma was detected typically for 72 h after a dose and in one subject for up to 120 h. Elimination of radioactivity from blood and plasma and of cold and radiolabeled deferasirox from plasma showed very similar mean half-lives of approximately 9.5 h (Table 1). Furthermore, Fig. 1 shows that concentrations of radioactivity and [¹⁴C]deferasirox were closely similar. Concentrations of the deferasirox iron complex in plasma at steady state, determined by a quantitative cold LC-UV assay, were low and showed no important time-dependent variation. No elimination half-life could be determined. Blood and plasma concentrations were subject to substantial interindividual variability. The S.D. data (Table 1) indicate that coefficients of variation were typically in a range from 40 to 60%.

Based on comparison of blood and plasma data, the radioactivity, which included deferasirox, the iron complex, and metabolite M3, was largely present in plasma. The mean radioactivity AUC ratio of blood versus plasma was 0.61 (Table 1). The distribution into red blood cells amounted to approximately 11%, which is similar to previous findings (Weiss et al., 2006).

Within the available data set (Table 1) it is interesting to compare AUC_{24 h} for various analytes at steady state and further to compare them with the AUC_(0-∞) for the single radiolabeled dose. As can be seen, the data were very consistent:

1. Comparison of the steady-state AUC_{24 h} (AUC_{ss}) of cold deferasirox versus single-dose radioactivity AUC showed a proportion of 87% (Table 1). Furthermore, the AUC_{24 h} of the complex (containing 2 molecules of deferasirox) accounted for approximately 10% of the plasma radioactivity AUC. Thus, the sum of the AUC_{ss} of deferasirox and of the iron complex approximately equals the total radioactivity AUC.
2. The AUC_{24 h} of [¹⁴C]deferasirox accounted for 91% of the radioactivity AUC_{24 h} (Table 1; Fig. 1), indicating that minimal amounts

TABLE 1

Pharmacokinetic parameters of ^{14}C radioactivity in blood and plasma and of [^{14}C]deferasirox, deferasirox at steady state, and deferasirox-iron complex at steady state in plasma

Data are means \pm S.D.; $n = 5$. Deferasirox and the complex were assayed by cold analysis, [^{14}C]deferasirox by radio-HPLC. Pharmacokinetic parameters represent apparent and descriptive data.

| Variable | Unit | Radioactivity | | [^{14}C]Deferasirox: Plasma ^a | Deferasirox (Steady State): Plasma | Complex (Steady State): Plasma |
|----------------------------------|--|-----------------|-----------------|---|------------------------------------|--------------------------------|
| | | Blood | Plasma | | | |
| t_{\max} (median) | h | 6 | 4 | 6 | 6 | 6 |
| C_{\max} | $\mu\text{mol/l}$ | 20.2 ± 10.6 | 32.7 ± 18.4 | 30.6 ± 15.7 | 46.5 ± 22.7 | 4.7 ± 3.0 |
| $\text{AUC}_{24\text{h}}$ | $\mu\text{mol} \cdot \text{h/l}^{b,c}$ | 292 ± 138 | 477 ± 229 | 434 ± 196 | 688 ± 307 | 79 ± 50 |
| | % ^{14}C -AUC _{24h} plasma | 61 ± 2 | (100) | 91 ± 6 | | |
| | % ^{14}C -AUC _{plasma} | | 60 ± 9 | | 87 ± 21 | 9.8 ± 5.2 |
| AUC_t | $\mu\text{mol} \cdot \text{h/l}^b$ | 434 ± 217 | 753 ± 351 | | | |
| t (median) | h | 48 | 72 | (24) | (24) | (24) |
| AUC | $\mu\text{mol} \cdot \text{h/l}^b$ | 459 ± 207 | 785 ± 355 | 710 ± 291^d | | |
| | % ^{14}C -AUC _{plasma} | 59 ± 4 | (100) | 91 ± 6 | | |
| $t_{1/2}$ | h | 12.2 ± 2.8 | 9.6 ± 4.0 | 11.0 ± 5.3 | 9.4 ± 3.6 | — ^e |
| Time interval (typical) | h | 12–48 | 12–48 | 8–24 | 8–24 | |
| Accumulation factor ^f | | | | | 1.60 ± 0.37 | |

^a [^{14}C]Deferasirox includes iron-complexed deferasirox. Under the conditions of the analytical system the radiolabeled complex cannot be measured separately.

^b $\text{AUC}_{24\text{h}}$ and AUC_t were calculated using the linear trapezoidal rule. $\text{AUC}_{t-\infty}$ was calculated as $C_t \cdot t_{1/2}/\ln 2$.

^c $\text{AUC}_{24\text{h}} = \text{AUC}_{ss}$ for (cold) deferasirox and complex.

^d Extrapolated from $\text{AUC}_{24\text{h}}$ using extrapolation factor 1.70 (from total ^{14}C).

^e Individual half-lives of 11 and 25 h were measured in two subjects.

^f $\text{AUC}_{ss}/\text{AUC}_{24\text{h}}$ of [^{14}C]deferasirox. Corrected for the complex included in [^{14}C]deferasirox the factor is 1.97 ± 0.57 .

of metabolites were present in the blood, apart from the iron complex.

- The accumulation factor of deferasirox was 1.60, determined as the ratio of deferasirox $\text{AUC}_{24\text{h}}$; [^{14}C]deferasirox $\text{AUC}_{24\text{h}}$ (Table 1). It has to be noted that the analysis for [^{14}C]deferasirox included the iron complex. Thus with correction for the complex, the accumulation factor was 1.97. This accumulation ratio was in the same range as observed in previous studies (Nisbet-Brown et al., 2003; Piga et al., 2006; Yang et al., 2007).
- Furthermore, in theory, AUC_{ss} of deferasirox and AUC of [^{14}C]deferasirox should be equal. A ratio of 1.09 was found. However, if the AUC of [^{14}C]deferasirox is corrected for the proportion of complex, the ratio is approximately 0.90.

Excretion and Mass Balance in Feces. Radiolabeled material was excreted largely in the feces (range 78.5–86.9% over 7 days) (Table 2). A minor proportion was excreted in urine with small interindividual variability (range 3.4–11.7% over 7 days). As a result, the mean total recovery in excreta over 7 days was 91.5% (range 90.2–92.7%).

Metabolite Characterization. The structures of the metabolites of [^{14}C]deferasirox were characterized by LC-MS with electrospray ionization in the positive ion mode. In-source fragmentation was used to generate fragment ions.

Hydroxy metabolites. The mass spectra of M1 and M4 in feces yielded mainly the molecular ion signal at m/z 390 (Table 3), an increase of 16 mass units compared with the $[\text{M} + \text{H}]^+$ peak in the mass spectrum of deferasirox. That suggested the introduction of one oxygen atom at an unknown position. The structures of the metabolites M1 and M4 (Fig. 2) were identified by comparison of retention

TABLE 2

Cumulative excretion of ^{14}C radioactivity in urine and feces after a single oral dose of 1000 mg of [^{14}C]deferasirox

Data are means \pm S.D.; $n = 5$.

| Time Period | Feces | Urine | Total |
|-------------|-----------------|---------------|-----------------|
| h | | % of dose | |
| 0–24 | 10.1 ± 17.8 | 5.1 ± 2.5 | 15.2 ± 20.2 |
| 0–72 | 80.2 ± 2.7 | 7.5 ± 2.9 | 87.7 ± 3.3 |
| 0–168 | 83.9 ± 3.1 | 7.6 ± 2.9 | 91.5 ± 1.1 |

times and mass spectra with those from the respective reference compounds NVP-AHN496 and NVP-AHN497 and with the metabolites identified in rat samples using detailed two-dimensional NMR analysis (Bruin et al., 2008). Two other possible hydroxylated metabolites M2 (3-OH) and M5 (3'-OH; numbering see structure formula in Table 3), known from several animal ADME studies, were not observed (Bruin et al., 2008).

Glucuronide conjugates. The mass spectra of metabolites M3 and M6 in urine showed the protonated intact molecule at m/z 550 (Table 3). A key fragment ($m/z = 374$, which equals m/z of protonated unchanged

TABLE 3

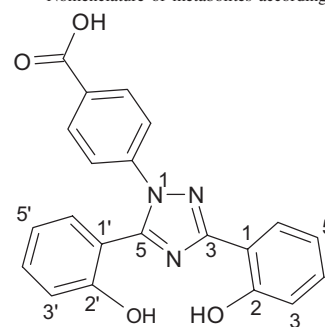
Mass spectrometry data and chemical identity of deferasirox metabolites in plasma, urine, and feces, based on LC/MS and comparison with reference metabolites

Mass spectrometry was performed with electrospray ionization and in source fragmentation at 25, 45, and 70 V (combined data).

| Component | Matrix | $[\text{M} + \text{H}]^+$ | Main Fragment | Assigned Structure ^a |
|-----------|--------|---------------------------|-------------------------|--|
| M1 | F | 390 | | NVP-AHN496 5-Hydroxy metabolite |
| M4 | F | 390 | | NVP-AHN497 5'-Hydroxy metabolite |
| M3 | U, P | 550 | 374 (–gluc) | Acyl glucuronide |
| M6 | U | 550 | 374 (–gluc) | 2-O-Glucuronide |
| M7 | U, F | 470 | 390 (–SO ₃) | 5-O-Sulfate |

P, plasma; U, native urine; F, feces extract; gluc, glucuronide.

^a Nomenclature of metabolites according to the following atom assignment in deferasirox:



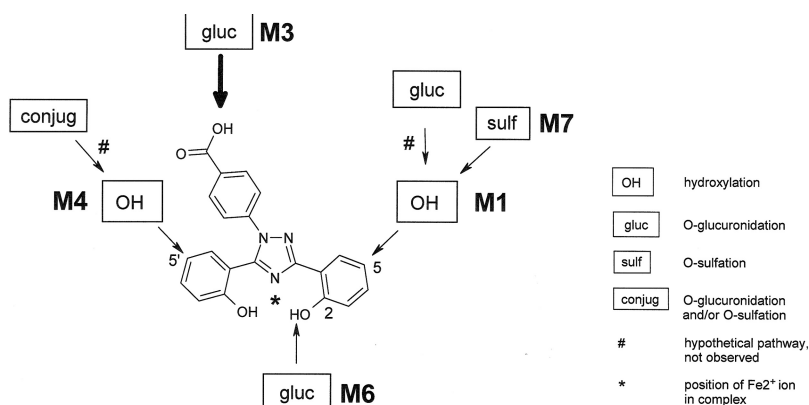


FIG. 2. Schematic chemical structures of deferasirox and its metabolites and identified metabolic pathways in human.

parent drug) showed the loss of a glucuronic acid moiety (-176 atomic mass units) in the MS spectrum of M3 and M6 and thus indicated the glucuronidation of unchanged deferasirox. Experiments in urine showed the disappearance of M3 and M6 after incubation with a β -glucuronidase/arylsulfatase enzyme mixture from *H. pomatia*. Comparison of the retention time of the glucuronide peak of approximately 29 min in this study with the retention time of the elucidated phenol *O*-glucuronide in urine from mice in a previous mouse ADME study confirmed M6 as the 2-*O*-glucuronide with conjugation in the phenol ring attached to the 3-position in the triazole ring (for numbering, see structure formula in Table 3). The instability of M3 observed at pH 10 and comparison of M3 in LC/MS with the acyl glucuronide identified in the rat ADME study (Bruin et al., 2008) confirmed that M3 was the acyl glucuronide of deferasirox. In the selected ion chromatograms at m/z 550, two additional peaks that closely migrated with the M3 peak were found. Those two additional peaks were not detectable in the radiochromatograms of urine. They probably represent arranged acyl glucuronides by intramolecular transesterification within the glucuronic acid moiety (Shipkova et al., 2003). "Acyl migration" in M3 was also observed in a previous rat ADME study (Bruin et al., 2008).

Sulfate conjugates. The mass spectrum of metabolite M7 present in feces in the positive ion mode yielded the molecular ion signal at m/z 470 with the main fragment at m/z 390 after the loss of 80 atomic mass units (Table 3). That is an indication of sulfate conjugation of one of the hydroxylated metabolites. M7, which was present in feces of four of five subjects, disappeared after incubation with β -glucuronidase/arylsulfatase with simultaneous formation of the hydroxy metabolite, M1. Therefore, M7 was identified as a sulfate conjugate of M1 (Fig. 2). Mass spectrometric investigation of urine also showed the presence of a sulfate conjugate of a hydroxylated metabolite. Cleavage experiments with the sulfate conjugate isolated from urine showed that it was the same sulfate conjugate M7.

Despite the somewhat different retention times of M7 in urine and feces, the analysis of a mixture of a urine sample and a feces sample extract confirmed that M7 represented the same conjugated metabolite in both matrices. Only one peak representing sulfate conjugate was observed, both in the radiochromatogram and in the selected ion chromatogram at m/z 470.

Metabolite Patterns. Most of the radioactivity in plasma was associated with unchanged deferasirox as can be seen in the chromatogram in Fig. 3. The deferasirox peak includes deferasirox involved in complex formation (under the conditions of the analytical system, the complex dissociates and cannot be measured). Systemic exposure to metabolites was minimal. Based on molecular mass and comparison with reference material, M3 was identified as the acyl glucuronide metabolite of deferasirox. No essential difference was

observed between patients. The mean plasma $AUC_{24\text{ h}}$ of M3 accounted for 3.3% of that of total radioactivity.

Metabolite patterns in pooled feces showed that a large dose fraction in feces was recovered as unchanged deferasirox. As with plasma, the deferasirox peak includes deferasirox involved in complex formation (under the conditions of the analytical system the complex dissociated and could not be measured). Based on LC-MS, enzymatic incubations, and comparison with reference material, M1, M3, M4, M6, and M7 were identified. There was no evidence of important interindividual differences in metabolism or elimination processes. Metabolite occurrence in urine and feces is summarized in Table 4. The data show moderate interindividual variability.

Metabolism in Human and Rat Hepatocytes In Vitro. In human hepatocytes [¹⁴C]deferasirox was predominantly metabolized to the acyl glucuronide (M3) by glucuronidation at the carboxylic acid moiety (Figs. 2 and 4). That result is in line with the levels of this metabolite in the systemic circulation, as reflected in plasma samples from the human in vivo study. In rat hepatocytes the formation of the acyl glucuronide (M3) was an important but not predominant pathway (Fig. 4).

In both species additional metabolic reactions of [¹⁴C]deferasirox were detected: 1) aromatic hydroxylation followed by subsequent sulfate conjugation yielding metabolite M7 (5-*O*-sulfate conjugate of M1) and 2) aromatic hydroxylation-forming metabolite M4 (5'-hydroxy metabolite of deferasirox). Phenolic glucuronidation with formation of metabolite M6 (2-*O*-glucuronide) was detected only in incubations with human hepatocytes. The formation of the acyl glucuronide of deferasirox was followed by subsequent migration of the acyl group from hydroxy position 1 to positions 2, 3, or 4 of the glucuronic acid moiety, yielding respective positional isomers of M3 (e.g., M3').

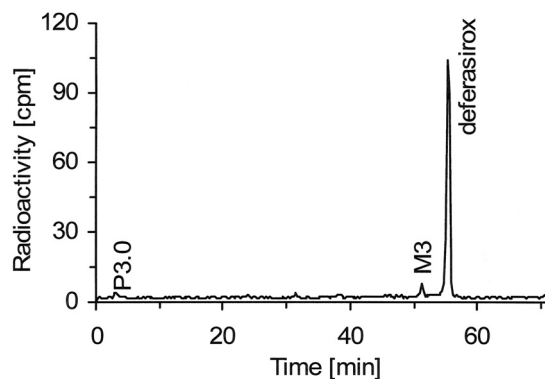


FIG. 3. Metabolite patterns in plasma of a representative subject at 4 h after dosing, by HPLC combined with microplate scintillation counting.

TABLE 4

Dose proportions of deferasirox and metabolites excreted in feces and urine

Data are means \pm S.D.; $n = 5$. Feces fractions 0 to 168 h and urine fractions 0 to 72 h were pooled.

| Compound | Feces | Urine | | Total |
|--|----------------|---------------|--|----------------|
| | | % dose | | |
| M1: 5-hydroxy metabolite of deferasirox | 4.4 \pm 2.6 | N.D. | | 4.4 \pm 2.6 |
| M3: acyl glucuronide of deferasirox | N.D. | 0.2 \pm 0.1 | | 0.2 \pm 0.1 |
| M4: 5'-hydroxy metabolite of deferasirox | 1.9 \pm 0.6 | N.D. | | 1.9 \pm 0.6 |
| M6: 2-O-glucuronide | N.D. | 6.3 \pm 2.9 | | 6.3 \pm 2.9 |
| M7: 5-O-sulfate conjugate of M1 | 2.0 \pm 2.4 | 0.3 \pm 0.1 | | 2.3 \pm 2.4 |
| Total of metabolites | 8.3 \pm 2.0 | 6.8 \pm 3.0 | | 15.1 \pm 4.5 |
| Deferasirox | 60.4 \pm 7.2 | 0.5 \pm 0.4 | | 60.9 \pm 7.4 |
| Not recovered from extraction and HPLC and unidentified traces | 14.4 \pm 8.4 | 0.2 \pm 0.2 | | 14.6 \pm 8.3 |
| Total of drug and metabolites | 83.1 \pm 4.0 | 7.5 \pm 2.9 | | 90.6 \pm 1.8 |

N.D., not detected.

In addition to comparison of retention times and mass spectra (as described before) the acyl glucuronidation was further confirmed in human hepatocyte incubations by enzymatic and alkaline hydrolysis. The disappearance of M3 and M6 but not of M3' was observed during incubation of the sample with a β -glucuronidase/arylsulfatase enzyme mixture from *H. pomatia*. At pH 10, M3 and M3' were unstable, but M6 was not. Therefore, it was concluded that M3 is the acyl glucuronide. M3' is probably an isomer of M3 formed by rearrangement of the acyl glucuronide by intramolecular trans-esterification (Shipkova et al., 2003).

Discussion

Absorption. From the results of this study, the absorbed dose proportion cannot be derived: renal excretion was low, there was little phase I metabolism, and hepatobiliary elimination of deferasirox, of iron complex, and of conjugates could not be measured, because no bile samples were obtained. In a clinical study in healthy volunteers, a mean oral absolute bioavailability of the final market image tablet formulation used in clinical studies was 70% (90% confidence interval: 62–80%) relative to an intravenous dose (Séchaud et al., 2008b). Thus, it is concluded that the gastrointestinal absorption was at least 70% if not close to complete. For comparison, the absorption in rats was 75% (Bruin et al., 2008).

Based on the t_{\max} values of 4 to 6 h observed in this study, the absorption process after dosing with a powder suspension formulation was slower than that with the established cold drug substance form (tablet suspension; t_{\max} 1–2 h) (Séchaud et al., 2008a). The composition of the formulations was the same for radiolabeled powder as for the nonradiolabeled tablet. It is not known whether there may have been any differences in the physicochemical properties of the drink suspensions formed in water. In a separate clinical study, it was shown that the degree of dispersion affected neither bioavailability of deferasirox nor t_{\max} (Séchaud et al., 2008a).

Pharmacokinetics in Plasma. The observed AUC values for deferasirox and the complex (single dose and steady state) were similar to those reported previously for the same dose level (20 mg/kg) (Nisbet-Brown et al., 2003; Piga et al., 2006).

In two of the five patients, the concentration-time curves in plasma showed a second, small concentration peak or "shoulder" at 24 h after dosing (approximately half of C_{\max}). That observation suggests some enterohepatic recirculation of deferasirox, which is consistent with previous observations in rats (Bruin et al., 2008) and results in other clinical studies (Galanello et al., 2008; Séchaud et al., 2008a,b). The extent of recycling cannot be determined from the available human data.

The predominant radiolabeled component in plasma was deferasirox (approximately 90% of AUC). Thus, systemic exposure was largely to deferasirox. Exposure to the deferasirox iron complex was 9 times lower. Metabolite M3 concentrations were minimal in the systemic circulation (3% of the ^{14}C -AUC), but M3 is assumed to have been an important terminal metabolite in the bile (see below).

Biotransformation. The extent and role of metabolism in the disposition of deferasirox can be assessed only from the metabolites in excreta, which represent the final result of drug elimination. However, in feces only phase I metabolites were found, with one minor exception. In the gut lumen, glucuronides are hydrolyzed by intestinal and/or microbial enzymes, leading to release of deferasirox or of the phase I metabolites, which are finally recovered in the feces. Therefore, without investigation of human bile, the glucuronides eliminated escape detection, the total amount of all metabolites formed and eliminated with bile cannot be determined, and the fecal metabolite balance substantially underestimates the true extent of metabolism. Most importantly, the acyl glucuronide of deferasirox (M3) is suspected to be formed in the liver and eliminated via bile as a main metabolite. This suspicion is based on two findings:

1. In complementary investigations in human hepatocytes, glucuronidation, particularly with formation of the acyl glucuronide (metabolite M3), was the major pathway, whereas in rat hepatocytes the formation of M3 was less important (Fig. 4).
2. In rats in vivo, M3 was the predominant metabolite in bile after oral and intravenous administration of [^{14}C]deferasirox (Bruin et al., 2008).

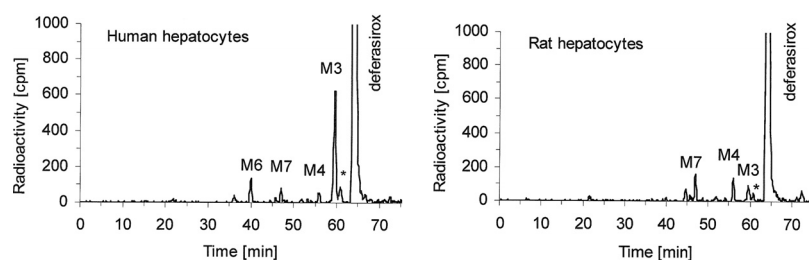


FIG. 4. Representative radio-HPLC profiles of [^{14}C]deferasirox (substrate concentration 50 μM , analysis of identical aliquots) and metabolites after 3-h incubations in the presence of human hepatocytes (left) or rat hepatocytes (right). *, indicates a metabolite (M3') formed by rearrangement of the acyl glucuronide M3 by intramolecular transesterification.

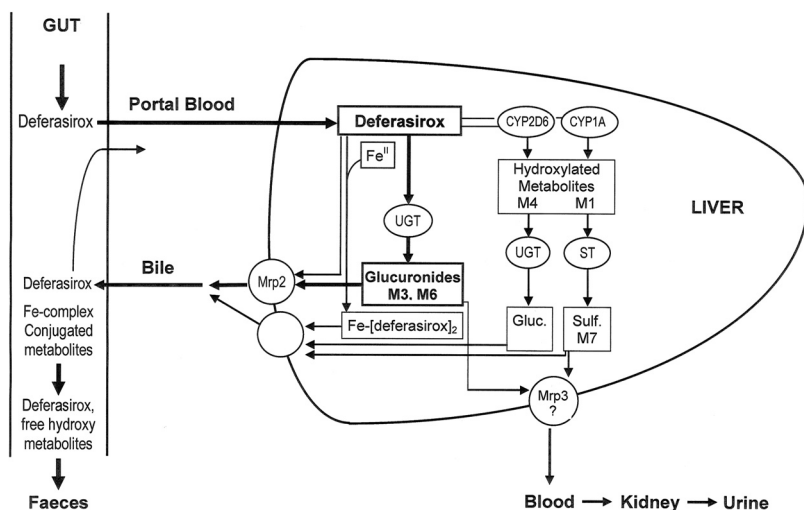


Fig. 5. Proposed scheme for the disposition of deferasirox in humans after peroral administration. ST, sulfotransferase; Gluc., glucuronic acid conjugate; Sulf., sulfate conjugate.

The combined results suggest that more M3 may be formed in human than in the rat and that M3 is, in fact, the main human metabolite. It should be added that M3 retains the structural elements and capability to form an iron complex and therefore might contribute to the elimination of iron via bile.

According to the above considerations, the dose fraction of approximately 60% excreted in the feces as unchanged deferasirox should not be misinterpreted as indicating low absorption or direct elimination. Unchanged deferasirox in feces most likely includes the following: 1) a small, unabsorbed fraction of the oral dose; 2) deferasirox, which was eliminated via bile, or secreted via the gut wall, partly due to first-pass elimination; and 3) the deferasirox glucuronides M3 and M6, which were eliminated via bile and deconjugated in the gut lumen.

P450-Catalyzed Metabolism. P450-catalyzed, oxidative metabolism of deferasirox seems not to be important in humans, as only 6% of dose was recovered in the form of the hydroxylated metabolites M1 and M7 and 2% as M4. M1 is formed by CYP1A and M4 by CYP2D6 (H. J. Einolf, R. Peter, L. Schofield, J. Chin, M. Shapiro, and H. Yin, unpublished data, Novartis). Therefore, neither inhibition nor induction of those enzymes by comedications nor genetic polymorphism (e.g., CYP2D6 poor metabolizer status) would be expected to significantly affect the pharmacokinetics of deferasirox.

Deferasirox weakly inhibited P450 activities with IC_{50} values ranging from 100 to $>500 \mu\text{M}$ (H. J. Einolf, R. Peter, and L. Schofield, unpublished data, Novartis). Given the relatively high therapeutic levels up to $50 \mu\text{M}$ at steady state, deferasirox might be suspected to inhibit CYP2C8, CYP1A2, CYP3A4/5, CYP2A6, or CYP2C9 and thus to interact with other drugs, although with the very high plasma protein binding of $>99.5\%$ (Weiss et al., 2006), significant inhibition by deferasirox is unlikely.

Mass Balance. The recovery of radioactivity was incomplete after 7 days, with a mean total excretion of $91.5 \pm 1.1\%$ of dose. At study end, daily excretion amounted to $<0.2\%$ of dose. It cannot be excluded that a dose proportion of approximately 8% remains retained in some organ(s) for a longer period and is eliminated very slowly. Based on organ distribution studies in rats, it appears likely that some residual radioactivity remained in the skin.

Elimination. From the study results and complementary data, we conclude that deferasirox is eliminated mainly by hepatic glucuronidation and hepatobiliary transport. Elimination by P450 enzyme-catalyzed hepatic phase I metabolism appears to contribute to a small extent. The elimination process is probably an anion transport, as

deferasirox and all metabolites are anions, with one or two negative charges. In vitro studies with human Caco-2 cell monolayers showed that deferasirox is a substrate of the anion transporter MRP2 (G. Camenisch, unpublished data, Novartis). Furthermore, studies in transport-deficient rats showed that MRP2 is involved in the hepatobiliary elimination of deferasirox and of the glucuronide M3 (Bruin et al., 2008). Because this transport system is well conserved across species (Cui et al., 1999; Bleasby et al., 2006), we conclude that the human MRP2 is involved in the elimination of deferasirox as well as its conjugated metabolites. The transporter that eliminates some deferasirox metabolites into the sinusoidal blood, from where it will be finally excreted via kidney, has not been investigated. A likely transporter is the basolateral MRP3 (Bruin et al., 2008). The results of this study and complementary data are compiled in Fig. 5, which is a schematic summary of the observed and/or proposed metabolism and elimination processes in liver and gut.

Acknowledgments. We acknowledge the valuable clinical support by Dr. Farrukh Shah (Whittington Hospital NHS Trust, London, UK), the sample analysis for drug levels by Dr. Stephane Delage (Novartis SA, Rueil-Malmaison, France), and the excellent technical assistance in metabolite analysis by Daniel Pierroz and Agnes Holler (Novartis, Basel, Switzerland). We thank Lesley Schofield and Drs. Heidi Einolf, Raimund Peter, and Gian Camenisch for providing results from P450 interaction and transporter studies and for helpful discussions.

References

- Barton JC (2007) Optimal management strategies for chronic iron overload. *Drugs* 67:685–700.
- Bleasby K, Castle JC, Roberts CJ, Cheng C, Bailey WJ, Sina JF, Kulkarni AV, Hafey MJ, Evers R, Johnson JM, et al. (2006) Expression profiles of 50 xenobiotic transporter genes in humans and pre-clinical species: a resource for investigations into drug disposition. *Xenobiotica* 36:963–988.
- Bruin GJ, Faller T, Wiegand H, Schweitzer A, Nick H, Schneider J, Boernsen KO, and Waldmeier F (2008) Pharmacokinetics, distribution, metabolism, and excretion of deferasirox and its iron complex in rats. *Drug Metab Dispos* 36:2523–2538.
- Bruin GJ, Waldmeier F, Boernsen KO, Pfaar U, Gross G, and Zollinger M (2006) A microplate scintillation counter as a radioactivity detector for high performance liquid chromatography in drug metabolism: validation and applications. *J Chromatogr A* 1133:184–194.
- Cui Y, König J, Buchholz JK, Spring H, Leier I, and Keppler D (1999) Drug resistance and ATP-dependent conjugate transport mediated by the apical multidrug resistance protein, MRP2, permanently expressed in human and canine cells. *Mol Pharmacol* 55:929–937.
- Galanello R, Piga A, Cappellini MD, Forni GL, Zappu A, Origa R, Dutreix C, Belleli R, Ford JM, Rivière GJ, et al. (2008) Effect of food, type of food, and time of food intake on deferasirox bioavailability: recommendations for an optimal deferasirox administration regimen. *J Clin Pharmacol* 48:428–435.
- Hinderling PH (1997) Red blood cells: a neglected compartment in pharmacokinetics and pharmacodynamics. *Pharmacol Rev* 49:279–295.
- Jost LM, Gschwind HP, Jalava T, Wang Y, Guenther C, Souppart C, Rottmann A, Denner K,

- Waldmeier F, Gross G, et al. (2006) Metabolism and disposition of vatalanib (PTK787/ZK-222584) in cancer patients. *Drug Metab Dispos* **34**:1817–1828.
- Kushner JP, Porter JP, Olivieri NF (2001) Secondary iron overload. *Hematology Am Soc Hematol Educ Program* **2001**:47–61.
- Nick H, Wong A, Acklin P, Faller B, Jin Y, Lattmann R, Sergejew T, Hauffe S, Thomas H, and Schnebli HP (2002) ICL670A: preclinical profile. *Adv Exp Med Biol* **509**:185–203.
- Nisbet-Brown E, Olivieri NF, Giardina PJ, Grady RW, Neufeld EJ, Séchaud R, Krebs-Brown AJ, Anderson JR, Alberti D, Sizer KC, et al. (2003) Effectiveness and safety of ICL670 in iron-loaded patients with thalassaemia: a randomised, double-blind, placebo-controlled, dose-escalation trial. *Lancet* **361**:1597–1602.
- Piga A, Galanello R, Forni GL, Cappellini MD, Origa R, Zappu A, Donato G, Bordone E, Lavagetto A, Zanaboni L, et al. (2006) Randomized phase II trial of deferasirox (Exjade, ICL670), a once-daily, orally-administered iron chelator, in comparison to deferoxamine in thalassemia patients with transfusional iron overload. *Haematologica* **91**:873–880.
- Rouan MC, Marfil F, Mangoni P, Séchaud R, Humbert H, and Maurer G (2001) Determination of a new oral iron chelator, ICL670, and its iron complex in plasma by high-performance liquid chromatography and ultraviolet detection. *J Chromatogr B Biosci Sci Appl* **755**:203–213.
- Séchaud R, Dutreix C, Balez S, Pommier F, Dumortier T, Morisson S, and Brun E (2008a) Relative bioavailability of deferasirox tablets administered without dispersion and dispersed in various drinks. *Int J Clin Pharmacol Ther* **46**:102–108.
- Séchaud R, Robeva A, Belleli R, and Balez S (2008b) Absolute oral bioavailability and disposition of deferasirox in healthy human subjects. *J Clin Pharmacol* **48**:919–925.
- Shipkova M, Armstrong VW, Oellerich M, and Wieland E (2003) Acyl glucuronide drug metabolites: toxicological and analytical implications. *Ther Drug Monit* **25**:1–16.
- Waldmeier F, Glaenzel U, Wirz B, Oberer L, Schmid D, Seiberling M, Valencia J, Riviere GJ, End P, and Vaidyanathan S (2007) Absorption, distribution, metabolism, and elimination of the direct rennin inhibitor aliskiren in healthy volunteers. *Drug Metab Dispos* **35**:1418–1428.
- Weiss HM, Fresneau M, Camenisch GP, Kretz O, and Gross G (2006) In vitro blood distribution and plasma protein binding of the iron chelator deferasirox (ICL670) and its iron complex Fe-[ICL670]₂ for rat, marmoset, rabbit, mouse, dog and human. *Drug Metab Dispos* **34**:971–975.
- Yang LP, Keam SJ, and Keating GM (2007) Deferasirox: a review of its use in the management of transfusional chronic iron overload. *Drugs* **67**:2211–2230.

Address correspondence to: Dr. Felix Waldmeier, Novartis Institutes for BioMedical Research—Drug Metabolism and Pharmacokinetics, Novartis Campus, WSJ-210.4.20, Postfach, CH-4056 Basel, Switzerland. E-mail: felix.waldmeier@novartis.com
